

See discussions, stats, and author profiles for this publication at: <https://www.researchgate.net/publication/231242928>

Rapid Solid-State Synthesis of Nanostructured Silicon

ARTICLE *in* CHEMISTRY OF MATERIALS · MARCH 2010

Impact Factor: 8.35 · DOI: 10.1021/cm903410s

CITATIONS

9

READS

17

8 AUTHORS, INCLUDING:



[Adam Makhuf](#)

University of California, Los Angeles

7 PUBLICATIONS 18 CITATIONS

[SEE PROFILE](#)



[Jean-Pierre Fleurial](#)

NASA

189 PUBLICATIONS 4,825 CITATIONS

[SEE PROFILE](#)

Rapid Solid-State Synthesis of Nanostructured Silicon

Sabah K. Bux,[†] Marc Rodriguez,[†] Michael T. Yeung,[†] Crystal Yang,[†] Adam Makhluf,[†]
Richard G. Blair,[‡] Jean-Pierre Fleurial,[§] and Richard B. Kaner^{*,†}

[†]Department of Chemistry and Biochemistry and California NanoSystems Institute, University of California, Los Angeles, 607 Charles E. Young Drive, Los Angeles, California 90095, [‡]Department of Chemistry, University of Central Florida, Orlando, Florida, and [§]Jet Propulsion Laboratory, California Institute of Technology, Pasadena, California 91109

Received November 8, 2009. Revised Manuscript Received February 23, 2010

Nanostructured silicon has recently been identified as an attractive material for a wide variety of uses from energy conversion and storage to biological applications. Here we present a new, rapid method of producing high-purity, nanostructured, unfunctionalized silicon via solid-state metathesis (SSM) in a matter of seconds. The silicon forms in a double displacement reaction between silicon tetraiodide and an alkaline earth silicide precursor. The products are characterized using powder X-ray diffraction, scanning electron microscopy (SEM), transmission electron microscopy (TEM), and energy-dispersive spectroscopy (EDS). Depending on the silicide precursor used, two different morphologies are obtained, either nanoparticles or dendritic nanowires. The variations in the morphologies are attributed to differences in the kinetics of the reactions.

Introduction

Nanostructured silicon has been utilized recently in a wide variety of applications from thermoelectrics,^{1–3} solar cells,⁴ and batteries⁵ to even biological imaging.⁶ Currently, there exist several methods for producing nanostructured Si including the pyrolysis of silane,⁷ pulsed laser ablation,⁸ MOCVD,¹ plasma etching,⁹ and electrochemistry.² However, these processes have inherent limitations, such as expensive and complex equipment and difficulty in scaling up reactions.

An alternate synthetic technique that can produce unfunctionalized nanostructured materials with good control over particle size is solid-state metathesis (SSM).¹⁰ SSMs are highly exothermic double displacement reactions, driven not only by the formation of the desired product but more importantly by the highly thermodynamically favorable

formation of salt. Most SSM reactions have been shown to rapidly reach or exceed temperatures of 1700 K in a matter of seconds. This very rapid heating can produce highly crystalline products.¹¹ Because the salt and product form simultaneously, a molten salt is created in which Ostwald ripening occurs uniformly, thus producing a relatively narrow particle size distribution of the product.¹² The salt is then washed away with water or acid, leaving behind the desired reaction product. SSM reactions have been used to produce a myriad of solid state compounds including borides,¹³ carbides,¹⁴ pnictides,^{15,16} and chalcogenides.¹⁷ Additionally, particle size can be controlled by the temperature of the reaction, which in turn can be controlled by adding inert material such as a salt to dissipate heat.¹² Previous work by Kauzlarich and co-workers produced monodisperse nanocrystalline silicon using solution-based metathesis.¹⁸ However, a capping ligand was needed to prevent particle agglomeration. This capping group, unless completely removed, can be problematic in applications such as thermoelectrics or solar cells, in which effective electron transfer is critical.

Described here are two SSM routes to the production of unfunctionalized nanocrystalline silicon. Phase-pure nanostructured silicon can be produced rapidly by reacting

*Corresponding author. E-mail: kaner@chem.ucla.edu.

- (1) Boukai, A. I.; Bunimovich, Y.; Tahir-Kheli, J.; Yu, J. K.; Goddard, W. A.; Heath, J. R. *Nature* **2008**, *451*(7175), 168–171.
- (2) Hochbaum, A. I.; Chen, R.; Delgado, R. D.; Liang, W.; Garnett, E. C.; Najarian, M.; Majumdar, A.; Yang, P. *Nature* **2008**, *451*(7175), 163–167.
- (3) Bux, S. K.; Blair, R. G.; Gogna, P. K.; Lee, H.; Chen, G.; Dresselhaus, M. S.; Kaner, R. B.; Fleurial, J.-P. *Adv. Funct. Mater.* **2009**, *19*(15), 2445–2452.
- (4) Tian, B.; Zheng, X.; Kempa, T. J.; Fang, Y.; Yu, N.; Yu, G.; Huang, J.; Lieber, C. M. *Nature* **2007**, *449*(7164), 885–889.
- (5) Chan, C. K.; Peng, H.; Liu, G.; McIlwrath, K.; Zhang, X. F.; Huggins, R. A.; Cui, Y. *Nat. Nanotechnol.* **2008**, *3*(1), 31–35.
- (6) Zhang, X. M.; Neiner, D.; Wang, S. Z.; Louie, A. Y.; Kauzlarich, S. M. *Nanotechnology* **2007**, *18*(9), 6.
- (7) Zhang, X.-Y.; Zhang, L.-D.; Meng, G.-W.; Li, G.-H.; Jin-Phillipp, N.-Y.; Phillipp, F. *Adv. Mater.* **2001**, *13*(16), 1238–1241.
- (8) Werwa, E.; Seraphin, A. A.; Chiu, L. A.; Zhou, C.; Kolenbrander, K. D. *Appl. Phys. Lett.* **1994**, *64*(14), 1821–1823.
- (9) Xu, S.; Levchenko, I.; Huang, S. Y.; Ostrikov, K. *Appl. Phys. Lett.* **2009**, *95*(11), 111505–3.
- (10) Gibson, K.; Ströbele, M.; Blaschkowski, B.; Glaser, J.; Weisser, M.; Srinivasan, R.; Kolb, H.-J.; Meyer, H.-J. *Z. Anorg. Allg. Chem.* **2003**, *629*(10), 1863–1870.

- (11) Gillan, E. G.; Kaner, R. B. *Chem. Mater.* **1996**, *8*(2), 333–343.
- (12) Janes, R. A.; Aldissi, M.; Kaner, R. B. *Chem. Mater.* **2003**, *15*(23), 4431–4435.
- (13) Rao, L. G.; E., G.; Kaner, R. B. *J. Mater. Res.* **1995**, *10*, 353–363.
- (14) Nartowski, A. M.; Parkin, I. P.; Craven, A. J.; MacKenzie, M. *Adv. Mater.* **1998**, *10*(10), 805–808.
- (15) Gillan, E. G.; Kaner, R. B. *Inorg. Chem.* **2002**, *33*(25), 5693–5700.
- (16) Treece, R. E.; Macala, G. S.; Rao, L.; Franke, D.; Eckert, H.; Kaner, R. B. *Inorg. Chem.* **2002**, *32*(12), 2745–2752.
- (17) Bonneau, P. R.; Jarvis, R. F.; Kaner, R. B. *Nature* **1991**, *349*(6309), 510–512.
- (18) Neiner, D.; Chiu, H. W.; Kauzlarich, S. M. *J. Am. Chem. Soc.* **2006**, *128*(34), 11016–11017.

silicon tetraiodide (SiI_4) with an alkaline earth metal silicide such as magnesium silicide (Mg_2Si) or calcium silicide (CaSi). The isolated Si product is characterized by powder X-ray diffraction, scanning electron microscopy, and transmission electron microscopy.

Experimental Section

Reagents. The following reagents were used in the synthesis of nanocrystalline silicon: SiI_4 (Alfa Aesar, 99%), CaSi (GFS Chemicals, 99.5%), CaSi_2 (Strem, 95%), and Mg_2Si (Cerac, 99.5%).

Synthesis. Stoichiometric mixtures of the precursor materials were ground to a homogeneous powder in an argon or helium filled glovebox. For reactions using the nichrome initiated method, the precursor amounts were measured in order to have a total precursor mass of 2 g (~ 0.25 g yield of the Si product via CaSi and CaSi_2 synthesis). The powders were then subjected to a resistively heated nichrome wire to initiate the reaction.

Warning: Solid-state metathesis reactions are extremely exothermic and may initiate upon grinding! Safety precautions should be taken prior to conducting these types of reactions or when scaling up. For mechanochemically initiated reactions, the precursor material total mass was scaled up to 8 g to yield 0.73 g of Si product via Mg_2Si and 1.25 g of Si product via CaSi reactions. The reactants were loaded into tungsten carbide vials with several tungsten carbide balls (SPEX CertiPrep Inc., Metuchen, NJ) and then loaded onto a Spex 8000D mixer mill (SPEX CertiPrep Inc., Metuchen, NJ) and milled for several hours. In the synthesis involving Mg_2Si and SiI_4 , the precursor materials were ball-milled to a homogeneous powder and the reaction was initiated using a drop of ethanol. **Warning:** Solid-state metathesis reactions are highly exothermic and should be handled in a fume hood or glovebox. This step involves the evolution of molecular iodine. The final products were washed with 50% 6 M HCl/50% ethanol to remove the salt byproduct, and then washed with ethanol and finally dried in air. All three of the reactions had more than 90% yield of the product.

Characterization. *Powder X-ray Diffraction.* The dried products were examined by powder X-ray diffraction (XRD) using a PANalytical Powder X-ray diffractometer using $\text{Cu K}\alpha$ ($\lambda = 1.5408 \text{ \AA}$) radiation. Scans were conducted with a range of $10^\circ \leq \theta \leq 100^\circ$ at 0.033° intervals and 25.13 s count times.

Scanning Electron Microscopy. Field emission scanning electron microscopy images were obtained with a JEOL JSM-6401F SEM and an FEI NOVA SEM operated with a 7–10 kV accelerating voltage.

Transmission Electron Microscopy. Nanosilicon samples were dispersed in ethanol and then pipetted onto a lacy carbon grid (SPI products). TEM imaging of the nanosilicon powders was performed on a FEI TF30UT TEM at 300 kV using a field-emission gun with an ultratwin lens. For imaging the Si nanowires, a FEI CM120 TEM at 300 kV using a field-emission gun was used.

Results

Powder X-ray diffraction was used to characterize the purity and crystallinity of the product. Figure 1 (bottom) and (top) shows a typical powder X-ray diffraction pattern (XRD) of the silicon product made from the CaSi and Mg_2Si precursors, respectively. The Miller indices for the highly crystalline diffraction peaks are presented in the figure, indicating an FCC lattice. No impurities were

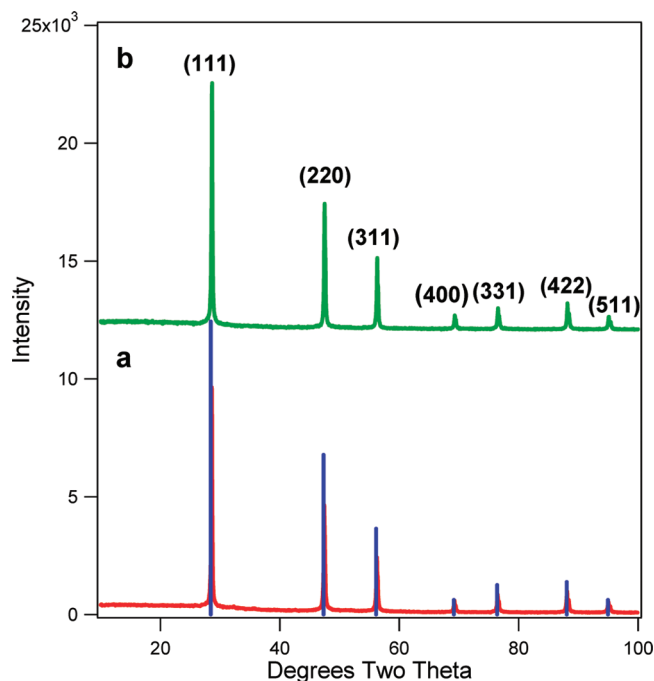


Figure 1. Powder X-ray diffraction patterns of nanostructured Si made from SiI_4 using (a) CaSi (bottom, red) and (b) Mg_2Si (top, green). The stick pattern overlay (blue) is the JCPDS file 00-027-1402 for silicon.

detected by XRD. However, when the CaSi_2 precursor is used, a significant amount of iron impurity (up to 5%) is detected. This can be attributed to the chemical production of CaSi_2 which is derived from wollastonite (CaSiO_3) or various forms of SiO_2 , all of which regularly contain iron impurities.^{19–21} The Williamson–Hall method of integral breadths was used to calculate the crystallite size assuming a spherical morphology.²² This method involves a linear plot of the width of a rectangle with the same height and area of each diffraction peak as a function of the d -spacing. The advantage of using this method is that both the crystallite size (the slope of the line) and the lattice strain (the y -intercept) can be calculated simultaneously without the use of an external standard. Using this method, the crystallite size for the CaSi -based product is 36 nm with a lattice strain of 0.112%. For the Mg_2Si -based product, the crystallite size is 39 nm with a lattice strain of 0.111%.

A scanning electron microscopy (SEM) image (Figure 2a) of the dried product from the reaction of SiI_4 and CaSi shows aggregates of Si nanoparticles ranging from submicrometer to micrometer sized particles. Energy-dispersive spectroscopy (EDS) (Figure 2b) confirms that the product is composed mainly of Si with some surface oxides and a slight Ca impurity. Figure 2c is the transmission electron microscopy (TEM) image

(19) De Chalmot, G. *Am. Chem. J.* **1896**, *18*, 319–321.

(20) Willson, T. L.; Haff, M. M. Production of Calcium Silicide. U.S. patent 934379, **1909**.

(21) Vaish, A. K.; Mahanty, M. S.; Saha, A. K.; Mathur, S. B.; Bodas, M. G.; Kumar, V.; Jana, R. K.; Khan, Z. H.; Bagchi, D. *NML Tech. J.* **1986**, *28*, 18–25.

(22) Klug, H. P.; Alexander, L. E. *X-ray Diffraction Procedures for Polycrystalline and Amorphous Materials*, 2nd ed.; John Wiley & Sons: New York, 1974.

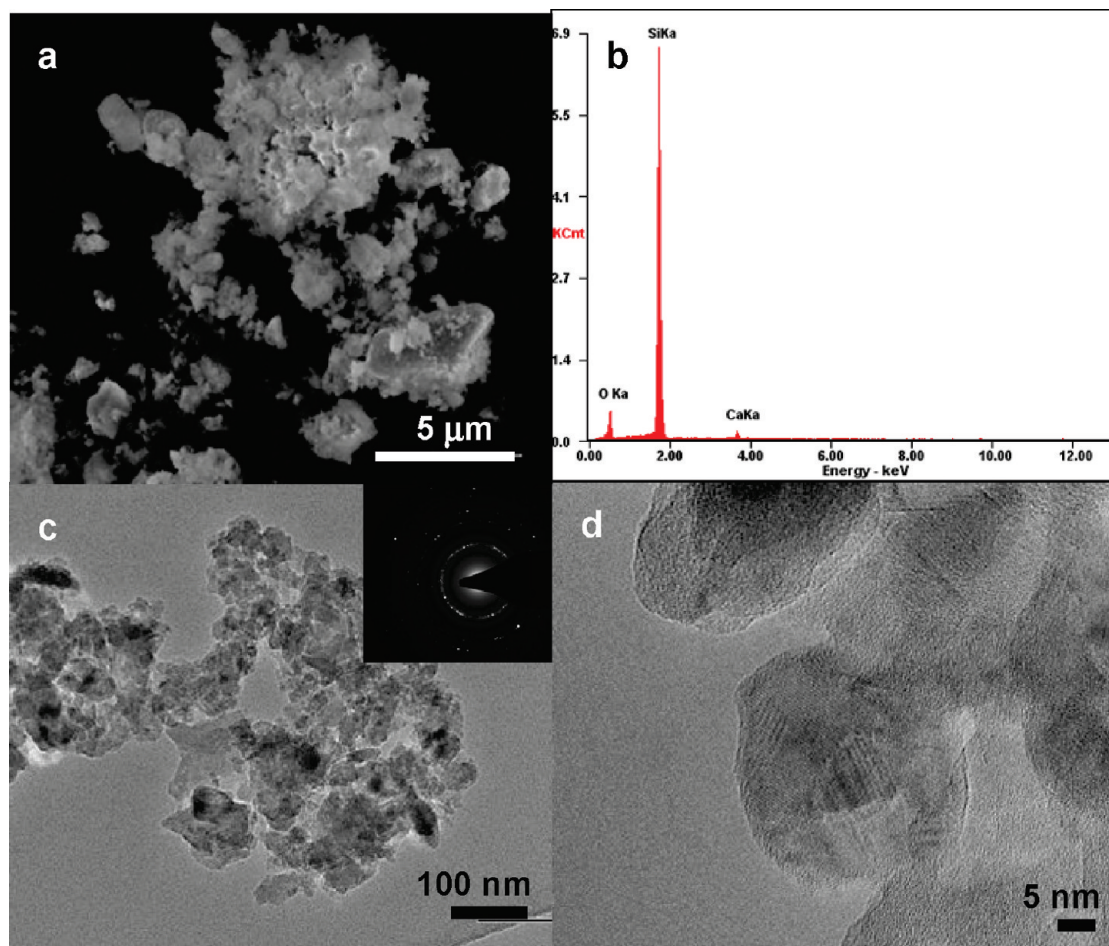


Figure 2. (a) SEM, (b) EDS, and (c) TEM images of nanostructured silicon produced using CaSi as the alkaline earth precursor. The TEM images show that the large particles seen in SEM are actually aggregates of smaller Si particles. Inset: Selected area electron diffraction pattern confirms that the product is nanocrystalline. (d) High-resolution TEM shows lattice fringes indicating that the large particles are made of smaller particles.

demonstrating that the large silicon nanoparticles are actually aggregates of smaller Si nanoparticles ranging from 30 to 50 nm in size, which is in agreement with the crystallite size calculated from XRD. The TEM diffraction pattern inset confirms that the Si nanoparticles are crystalline in nature.

When the alkaline earth silicide precursor is changed from CaSi to Mg_2Si , there is a significant change in the morphology of the nanostructured Si product. A SEM image (Figure 3a) shows nanowire bundles, several micrometers in size that resemble groups of oriented dendritic wires comprised of nanowires with diameters of approximately 50 nm. A transmission electron microscopy (TEM) image (Figure 3c) shows that the Si nanowires are 40 nm in diameter with a 10 nm thick oxide layer, which is in agreement with the crystallite size calculated from XRD. Selected area electron diffraction (SAED) (Figure 3d) of the nanowires demonstrates that they are highly crystalline with a diffraction pattern oriented generally along the 111 direction.

Earlier work by Janes and co-workers demonstrated that the crystallite size of the product of a metathesis reaction can be controlled by the addition of an inert salt diluent, which acts as a heat sink retarding Oswald ripening.¹² A similar study was conducted here by using

sodium chloride (NaCl) as the inert salt diluent

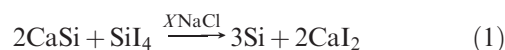


Figure 4 shows that with increasing salt concentration (X), the crystallite size decreases significantly from 36 nm down to about 12 nm. The addition of the inert salt acts as an aid to prevent grain coarsening and Oswald ripening by acting as a heat sink. This is reflected in the decreased calculated maximum adiabatic temperature from 2050 to 1555 K as result of the NaCl addition (see Figure 4 and Table 1).

To form the Si nanowires, we used a drop of ethanol to initiate the reaction. Figure 5 shows time-elapsd photography of a $\text{Mg}_2\text{Si} + \text{SiI}_4$ reaction. The ethanol droplet initiates the reaction, and in less than 1 min, the reaction reaches completion.

Discussion

The idealized reactions between silicon tetraiodide and the alkaline earth silicide precursors are as follows



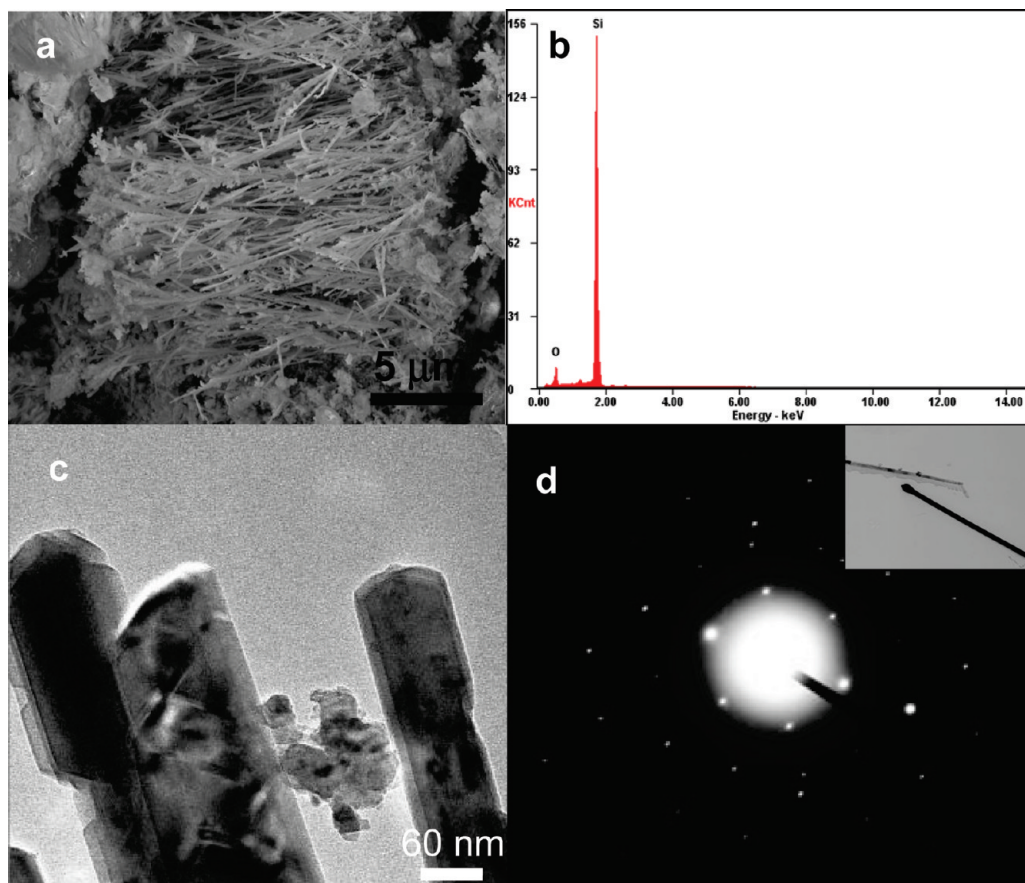


Figure 3. (a) SEM image. (b) EDAX of the product produced from the reaction of SiI_4 with Mg_2Si . The Si nanowires average 50 nm in diameter and the product is mainly Si with some oxygen and residual Mg. (c) TEM image of the Si nanowires; the lighter area is believed to correspond to a 10 nm thick oxide layer on the nanowires. (d) SAED pattern of the nanowires showing that they grow in the (111) direction.

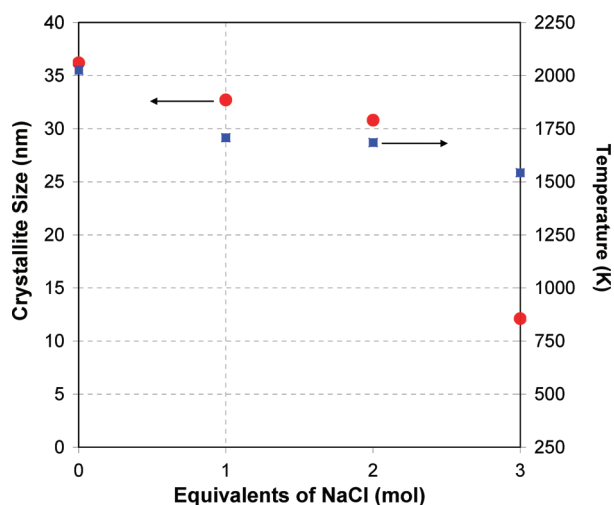


Figure 4. Crystallite size (circles) and calculated maximum adiabatic temperature (squares) as a function of NaCl mole addition (X) according to the reaction of $\text{SiI}_4 + 2\text{CaSi}$. NaCl reduces the maximum adiabatic temperature by acting as a heat sink and thus retarding Oswald ripening, which keeps the crystallites small.

Because metathesis reactions are thermodynamically driven, the enthalpy of formation can be calculated using standard thermodynamic values and are -689.9 and -289.0 kJ/mol for the CaSi and Mg_2Si reactions, respectively. The calculated maximum adiabatic temperatures of the reactions are determined to be 2025 K for the CaSi

Table 1. Calculated Crystallite Size and Temperature Reduction for Nanostructured Silicon Produced by the Reaction between CaSi and SiI_4 with Increasing Molar Equivalents of NaCl

equivalents of NaCl (mol)	crystallite size (nm)	T (K)
0	36.2	2025
1	32.7	1708
2	30.8	1685
3	12.1	1543

reaction and 1254 K for the Mg_2Si reaction. These temperatures are calculated assuming complete reactions with no heat loss.²³ These temperatures correspond to the boiling points²⁴ of the respective salts. The SSM reactions can either be initiated using a resistively heated nichrome wire or mechanochemically using a high energy ball mill. For the CaSi -based reaction, both initiation methods yielded similar morphologies and crystallite sizes.

The use of high-energy ball-milling was investigated as a method for safely containing the precursor materials while scaling the reactions up from 2 g total reactant mass for the nichrome initiated method to an 8 g reactant scale. The ball-milling method has received a great deal of attention recently in the synthesis of thermoelectric materials.³ The nanoscale materials are produced by the

(23) Rao, L.; Yu, P.; Kaner, R. B. *J. Mater. Synth. Process.* **1994**, 2(6), 343–353.

(24) Barin, I., *Thermochemical Data of Pure Substances*; Verlagsgesellschaft mbH: Weinheim, Germany, 1993; Vols. 1 and 2.

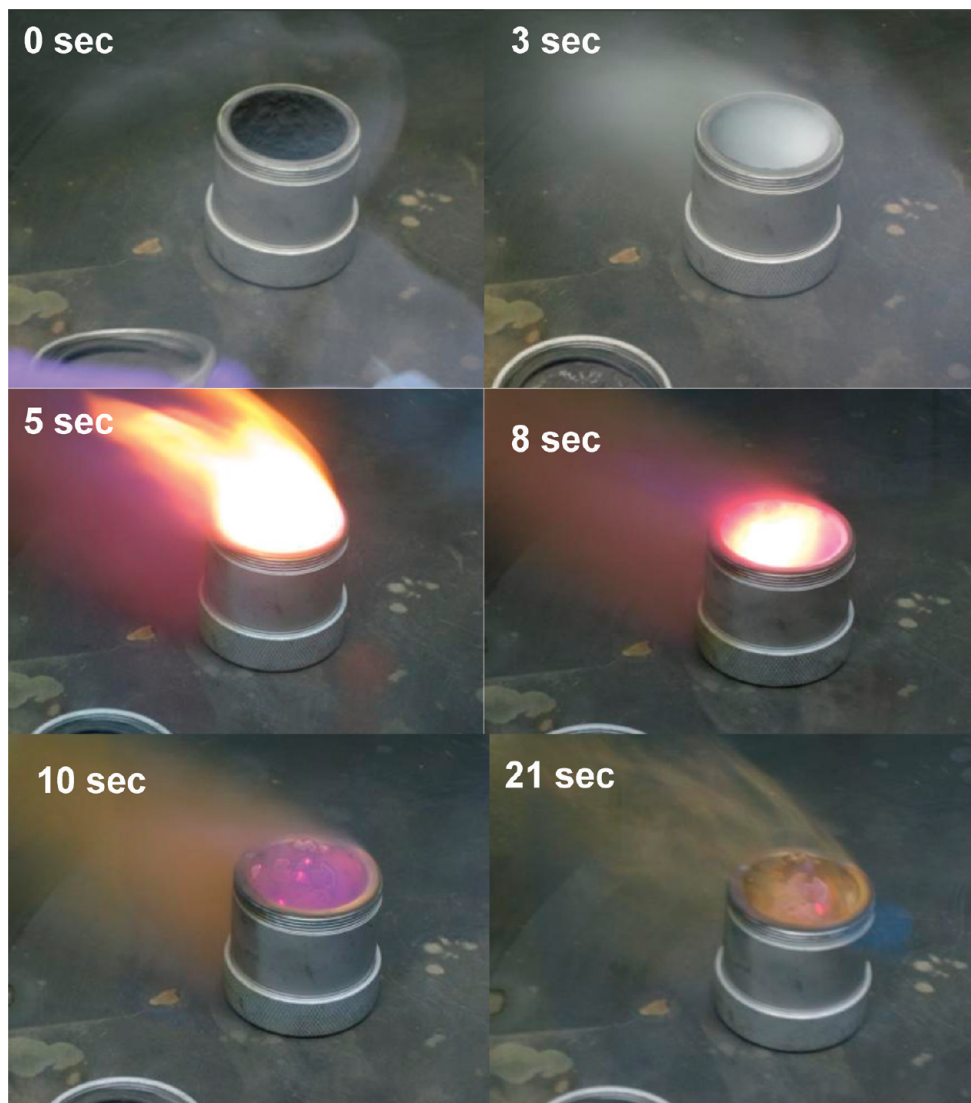


Figure 5. Time lapse photography of the reaction of Mg_2Si and SiI_4 initiated by a drop of ethanol. A large violet plume of iodine vapor is observed approximately 5 s into the reaction. **Warning:** Solid-state metathesis reactions are highly exothermic and should be handled in a fume hood or glovebox. This step involves the evolution of molecular iodine.

constant fracturing and cold welding of the powders during the milling process. Additionally, it has been demonstrated that the mechanical work of the ball-milling process can directly initiate chemical reactions.^{25,26} Moreover, using ball-milling ensures that all of the reactants are consumed in the reaction by continuously injecting energy into the reaction. This differs from scaling up nichrome wire-initiated metathesis reactions that may have variations in yield and morphologies of the product because of changes in the kinetics.

Janes and co-workers¹² demonstrated that the temperature and crystallite size can be controlled by the addition of an inert diluent such as NaCl. Here, different molar equivalents of NaCl were added to the CaSi based reaction (Table 1 and Figure 4). The addition of the salt

serves to retard Oswald ripening by decreasing the reaction temperature, therefore reducing the nucleation and growth time for the nanoparticles, by absorbing some of the heat of the reaction. The NaCl dissipates the heat of the reaction by causing the increasingly rapid reaction temperature to slow at 1074 K (the melting point of NaCl) and more significantly at 1686 K (the boiling point of NaCl) since the enthalpy of boiling NaCl is quite large (188 kJ/mol).²⁷ In the reaction between CaSi and SiI_4 , the reaction enthalpy (-689 kJ/mol) is sufficiently high that the maximum adiabatic temperature (2025 K) exceeds the boiling point of NaCl. By adding more salt, the crystallite size of the silicon decreases from 36 to 12 nm. Concurrently, the maximum adiabatic temperature also decreases from 2050 to 1555 K, at which point the reaction no longer propagates. This can be attributed to incomplete heat distribution, likely leading to incomplete melting of the salt, which in turn prevents propagation as

(25) Cook, B. A.; Beaudry, B. J.; Harringa, J. L.; Barnett, W. J. *Proceedings of the 24th Intersociety Energy Conversion Engineering Conference*; Arlington, VA, August 1989; IEEE: Piscataway, NJ, 1989; pp 693–700 vol.2.

(26) Hick, S. M.; Griebel, C.; Blair, R. G. *Inorg. Chem.* **2009**, 48(5), 2333–2338.

(27) Borucka, A. Z.; Bockris, J. O. M.; Kitchener, J. A. *Proc. R. Soc. London, Ser. A* **1957**, 241(1227), 554–567.

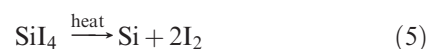
discussed in an earlier article.¹² Additional heating and milling were attempted to try to force the reaction to propagate, without success. When the NaCl was added to the Mg₂Si reaction, the dendritic nanowire morphology was lost. The reaction between Mg₂Si and SiI₄ is much less exothermic (−289 kJ/mol) and the maximum adiabatic temperature does not reach the boiling point of NaCl, but only just exceeds its melting point (1074 K). Therefore, the Si produced from the reaction of Mg₂Si and SiI₄ grows for a longer time in the molten salt because of Oswald ripening and loses its dendritic morphology.

Figures 2 and 3 show a remarkable difference in the morphologies of the nanostructured silicon depending on which precursor is used. Although metathesis reactions reach completion in a matter of seconds, it is not unprecedented to have such ordered and complex structures being formed in situ, as is the case in the formation of carbon nanotubes via metathesis.²⁸ The morphological changes can be attributed to the difference in the decomposition temperatures and maximum adiabatic temperatures for the CaSi and Mg₂Si precursors and the favorable formation of the salts. CaSi decomposes at a temperature of 1473 K²⁹ and its reaction reaches a maximum adiabatic temperature of 2025 K, whereas Mg₂Si decomposes at 1358 K and its reaction reaches a maximum adiabatic temperature of 1254 K. These temperatures are directly related to the exothermic nature of the metathesis reactions (CaSi + SiI₄ = −698 kJ/mol, Mg₂Si + SiI₄ = −298 kJ/mol). As a result of the lower decomposition temperature and smaller enthalpy of formation for Mg₂Si + SiI₄, the energy transfer kinetics are fast, whereas the mass transfer kinetics are much slower, thereby allowing time for nanowires to grow. Kinetic studies of metathesis reactions have been quite difficult, since the reactions occur rapidly and reach such high temperatures in a matter of seconds. Earlier attempts to examine metathesis reactions spectroscopically were derailed by the intense blackbody radiation from the reaction that is evident 5 s into the reaction (Figure 5, frame 3). To obtain insight into the reaction mechanism, we investigated studies involving different reaction conditions and their impact on the products.

To create the Si nanowires, we used a drop of ethanol to initiate the reaction. **Warning:** *Solid-state metathesis reactions are highly exothermic and should be handled in a fume hood or glovebox. This step involves the evolution of molecular iodine.* The nanowire mechanism is speculated to be a two-step mass transfer kinetic process. The first step involves the ethanol droplet reacting with the high-surface-area Mg₂Si precursor to oxidize it to MgO and SiH₄ (eq 4)



The heat that is released from the oxidation of Mg₂Si to MgO and the combustion of silane and acetylene in turn decomposes the SiI₄ into Si and I₂ (eq 5)



The I₂ can then act as a vapor transport agent, forming nanowires on the cool walls of the container. Evidence for iodine vapor is provided by the violet colored plume emanating from the reaction vial five seconds after the reaction is initiated (Figure 5). The violet plume was confirmed to be iodine by conducting a starch-iodine test.³⁰

Ethanol is believed to play a crucial role in the process of forming the nanowires. The use of an aqueous phase to initiate a metathesis reaction was first reported by Bonneau, et al., in which the use of a hydrated precursor material was critical to the success of a metathesis reaction between potassium hexafluoronickelate(IV) and sodium pentasulfide hydrate.³¹ Because all solid-state reactions are limited by the rate of solid–solid diffusion, the ethanol molecule facilitates the metathesis reaction by interacting with the reactive Mg₂Si precursor. When ethanol is substituted with a more reactive and stronger oxidizing agent, such as 6.0 M hydrochloric acid, the silicon is rapidly oxidized and amorphous SiO₂ is formed. However, if a branched alcohol such as isopropanol is used, the reaction does not propagate and the precursor materials remain largely intact. When the reaction is initiated using a water-free solvent, such as dimethylformamide under inert conditions, very few nanowires are obtained, suggesting that oxygen plays a crucial role in the formation of nanowires. Although the precise role of oxygen is not known, several studies suggest that oxygen facilitates nanowire formation.^{32–34} Note that the ball-milling process does not initiate the reaction but serves to produce a powder with a high surface area³⁵ suitable for initiating the desired reaction with a drop of ethanol.

Conclusions

A new, rapid, solid-state metathesis route to produce highly crystalline, unfunctionalized nanostructured silicon from reactive alkaline earth silicides and silicon tetrahalides has been developed. Depending on the silicide precursor that is used, two different Si morphologies can be achieved. When the CaSi precursor is used, an aggregated particulate morphology is obtained; however, with the Mg₂Si precursor, nanowires are created. The differences in the morphologies are attributed to the differences in the kinetics of the reactions after initiation. The particle size can be controlled by simply adding an inert diluent which acts as a heat sink.

(28) Mack, J. J.; Tari, S.; Kaner, R. B. *Inorg. Chem.* **2006**, 45(10), 4243–4246.

(29) Manfrinetti, P.; Fornasini, M. L.; Palenzona, A. *Intermetallics* **2000**, 8(3), 223–228.

(30) Ebbing, D. D.; Gammon, Steven D. *General Chemistry*, 6th ed.; Houghton Mifflin Company: Boston, 1999.

(31) Bonneau, P. R.; Shibao, R. K.; Kaner, R. B. *Inorg. Chem.* **1990**, 29(13), 2511–2514.

(32) Kodambaka, S.; Hannon, J. B.; Tromp, R. M.; Ross, F. M. *Nano Lett.* **2006**, 6(6), 1292–1296.

(33) de Vasconcelos, E. A.; dos Santos, F. R. P.; da Silva, E. F.; Boudinov, H. *Appl. Surf. Sci.* **2006**, 252(15), 5572–5574.

(34) Levchenko, I.; Cvelbar, U.; Ostrikov, K. *Appl. Phys. Lett.* **2009**, 95(2), 021502–3.

(35) Farhat, Z.; Alfantazi, A. *Mater. Sci. Eng., A* **2008**, 476(1–2), 169–173.

Acknowledgment. The authors thank Dr. Thierry Caillat, Daniel King, and Kurt Star their helpful discussions and Veronica Strong and Sergey Prikhodko for their assistance with TEM and SAED. Support from the National Science Foundation DMR 0805352 (R.B.K.), an IGERT fellowship DGE-0114443 and DGE-0654431 (S.K.B.), a NASA GSRP

fellowship NNX09AM26H (S.K.B.), and a JPL/Caltech subcontract 1308818 (R.B.K.) are gratefully acknowledged. Part of this work was performed at the Jet Propulsion Laboratory, California Institute of Technology under contract with the National Aeronautics and Space Administration.